Ectopic Expression of Syncollin in INS-1 β-Cells Sorts It into Granules and Impairs Regulated Secretion†

Jingsong Li,‡ Ruihua Luo,‡ Shing Chuan Hooi,§ Pilar Ruga,|| Jiping Zhang,‡ Paolo Meda,⊥ and GuoDong Li*,‡

Cardiovascular Research Institute, National University Medical Institutes, and Department of Physiology, National University of Singapore, Singapore, and Pole Facultaire de Microscopie Ultrastructurale, CMU, and Department of Cell Physiology and Metabolism, University of Geneva, 1211 Genève 4, Switzerland

Received May 30, 2004; Revised Manuscript Received January 2, 2005

ABSTRACT: Syncollin was first demonstrated to be a protein capable of affecting granule fusion in a cell-free system, but later studies revealed its luminal localization in zymogen granules. To determine its possible role in exocytosis in the intact cell, syncollin and a truncated form of the protein (lacking the N-terminal hydrophobic domain) were stably transfected in insulin-secreting INS-1 cells since these well-studied exocytotic cells appear not to express the protein per se. Studies by subcellular fractionation analysis, double immunofluorescence staining, and electron microscopy examination revealed that transfection of syncollin produced strong signals in the insulin secretory granules, whereas the product from transfecting the truncated syncollin was predominantly associated with the Golgi apparatus and to a lesser degree with the endoplasmic reticulum. The expressed products were associated with membranes and not the soluble fractions in either cytoplasm or the lumens of organelles. Importantly, insulin release stimulated by various secretagogues was severely impaired in cells expressing syncollin, but not affected by expressing truncated syncollin. Transfection of syncollin appeared not to impede insulin biosynthesis and processing, since cellular contents of proinsulin and insulin and the number of secretory granules were not altered. In addition, the early signals (membrane depolarization and Ca^{2+} responses) for regulated insulin secretion were unaffected. These findings indicate that syncollin may be targeted to insulin secretory granules specifically and impair regulated secretion at a distal stage.

Syncollin was initially identified as a syntaxin-binding protein in pancreatic exocrine acinar cells (*1*). Introduction of this protein in a cell-free exocytosis system affected the fusion of isolated secretory granules with the plasma membrane, an effect mediated by its interaction with syntaxin in a Ca^{2+}-dependent manner (*1*). However, the significance of such an action became questionable, since subsequent work found that endogenous syncollin in exocrine pancreatic acinar cells seems to be a luminal protein in zymogen granules and its physiological function remains unclear (*1*−*3*). Expression of this protein was also observed in small intestine and parotid gland (*1*, *2*, *4*). Interestingly, our previous work found that its expression in small intestine is regulated by feeding (*2*), suggesting a potential role in the regulation of digestive enzymes.

The gene for full-length rat syncollin expresses a protein of 134 amino acids with a hydrophobic domain at its N-terminus (*2*, *5*). On the other hand, the sequence of this hydrophobic domain also meets the criteria for a signal peptide and thus may function to direct the synthesized peptide into the endoplasmic reticulum (ER) lumen to form secretory proteins or ER chaperones (*5*). A truncated form of syncollin lacking this domain may cause mistargeting and loss of normal function.

In view of its effect on the exocytotic process in vitro and the failure to detect syncollin in the pancreatic β-cell, we made use of this cell system to determine the possible role of syncollin (or its homologue proteins) in regulated secretion in intact cells. In this study, syncollin and its truncated form (lacking the N-terminal hydrophobic domain) were stably expressed in the insulin-secreting β-cell line (INS-1), a widely studied exocytotic cell system (*6*, *7*). Our results have demonstrated that insulin secretory responses to various secretagogues were markedly impaired in cells transfected with syncollin, but not in cells transfected with truncated syncollin. Subcellular fractionation analyses and immunofluorescence staining revealed that the expressed products from both forms of syncollin vectors displayed a similar molecular mass and were exclusively associated with membrane-containing structures. However, their subcellular localization was different. Expression of the syncollin vector produced a protein that was identified in the secretory granule-enriched fraction and colocalized with insulin. In

† This work was supported by grants (NMRC/0540/2001 and NMRC/0803/2003) from the National Medical Research Council of Singapore (to G.L.). P.M.'s team was supported by grants from the Swiss National Science Foundation (31-67788.02), the Juvenile Diabetes Research Foundation International (1-2005-46 and 5-2004-255), the European Union (QLRT-2001-01777), and the National Institutes of Health (1RO1 DK-63443-01). J.L. is a recipient of Research Scholarship from the National University of Singapore.

* To whom correspondence should be addressed: National University Medical Institutes, Blk MD11 #02-01, 10 Medical Dr., Singapore 117597. Telephone: (65) 6874 5188. Fax: (65) 6773 5461. E-mail: nmiligd@nus.edu.sg.

‡ National University Medical Institutes.

§ National University of Singapore.

|| CMU.

⊥ University of Geneva.

10.1021/bi048894d CCC: $30.25
Published on Web 02/25/2005

contrast, the product from transfection of the truncated syncollin construct was detected predominantly in the microsomal fraction and colocalized with the markers of the Golgi apparatus and ER.

MATERIALS AND METHODS

Plasmids and Antiserum. The gene for syncollin was isolated and cloned from rat (*Rattus norvegicus*) duodenum by utilizing a subtractive hybridization strategy in one of our laboratories (*2*). The two plasmids containing rat syncollin or its truncated form [lacking the N-terminal hydrophobic domain of 19 amino acids (MSPLCLLLLA-LALVAVPGA)] were constructed by cloning them into the pCDNA 3.1A vector (from Clontech) by RT-PCR (the underlined regions in primers refer to restriction sites), in which 5′-ccggaattaccatgtccccgctgtgcct-3′ and 5′-ccggaatttcaat-agcacttgcagtaga-3′ were used as forward and reverse primers for syncollin, respectively, while 5′-ccggaattcaccatgcgag-gcgcttgtccagtgcc-3′ and 5′-ccggaatttcaatagcacttgcagtaga-3′ were used as forward and reverse primers for the truncated syncollin, respectively. The PCR products were digested with EcoRI and ligated to the vector by T_4 DNA ligase (Promega) followed by transformation to *Escherichia coli* XL1blue. Positive clones were confirmed by sequencing. An empty vector was used as a control plasmid. The full-length syncollin construct encodes from amino acid Met (residue 1) to amino acid Tyr (residue 134, before the termination code), whereas the truncated syncollin construct encodes from amino acid Arg (residue 20) to terminal amino acid Tyr (residue 134). Myc-tagged syncollin was constructed by cloning the intact syncollin gene or its truncated form in pCDNA 3.1A without terminal codes. Plasmids were amplified in *E. coli* XL1blue and purified by using a Midi-prep plasmid kit (Bio-Rad). The anti-syncollin antiserum (customer-ordered from GeneMed Synthesis, Inc.) was raised in rabbits by injecting a synthesized 16-residue peptide of rat syncollin (KRGKTRKFSTGSYPRC, residues 96−108) conjugated with KLH (keyhole limpet hemocyanin) at the N-terminus.

Cell Culture and Transfection. INS-1 cells (passage 56−75; a gift from C. B. Wollheim, University of Geneva) were grown in RPMI 1640 (Sigma) containing 10% fetal calf serum (GIBCO BRL), 50 μM 2-mercaptoethanol, and 1 mM pyruvate in culture flasks (Falcon) at 5% CO_2 (*6*). For transfection, cells seeded in six-well plates (Falcon) were cultured for 1 day to reach 80% confluence. Transfection was conducted by using Fugene-6 reagent according to the manufacturer's protocols (Roche Diagnostics). One microgram of purified plasmid DNA was applied to each well. Control cells were transfected by incubation with an equivalent amount of empty vector DNA. Stably expressing cells were established by selecting transfected cells with 50 μg/mL G418 (Sigma) for 4 weeks, followed by confirmation with a Western blotting assay for syncollin in cell lysates.

Subcellular Fractionation. Subcellular fractions of INS-1 cells were isolated as previously described (*8*). All procedures were performed on ice. Approximately 4.5×10^7 cells grown in 15 cm culture dishes (Falcon) were washed twice with cold PBS and scraped in 1 mL of homogenization buffer [20 mM Tris-HCl (pH 7.4), 0.5 mM EDTA, 0.5 mM EGTA, 250 mM sucrose, and 1 mM dithiothreitol] containing the following protease inhibitors: leupeptin (10 μg/mL), aprotinin (4 μg/mL), pepstatin (2 μg/mL), and PMSF (100 μM). The cells were then disrupted by 10 strokes through a 27 gauge needle. The cell homogenates were centrifuged at 900*g* for 10 min to remove the nuclei and unbroken cells. Mitochondria-enriched, secretory granule-enriched, and microsomal fractions were harvested by centrifuging post-nuclear supernatants in an Eppendorf centrifuge at 5500*g* for 15 min, in a Beckman L-80 ultracentrifuge at 25000*g* for 20 min, and in a Beckman L-80 ultracentrifuge at 100000*g* for 60 min, respectively. For plasma membrane isolation (*9*), the cell homogenates were centrifuged at 280*g* for 5 min to remove the nuclei and unbroken cells. The pellets were resuspended in 1 mL of medium A [0.25 M sucrose, 1 mM $MgCl_2$, and 10 mM Tris-HCl (pH 7.4)] and mixed well with 2 volumes of medium B [2 M sucrose, 1 mM $MgCl_2$, and 10 mM Tris-HCl (pH 7.4)]. The mixture was overlaid with 0.5 mL of medium A, and the tubes were centrifuged at 113000*g* for 1 h. A band at the interface containing the plasma membrane was collected and diluted to 2 mL with the homogenization buffer. The pellets were harvested after centrifugation at 3000*g* for 10 min. It has been demonstrated that this practice generates a highly purified plasma membrane fraction with only 4.6, 1.5, and 20% of contamination from mitochondria, lysosomes, and ER, respectively (*10*). Protein concentrations in subcellular fractions were measured using a Bio-Rad assay kit.

In another series of experiments assessing the location of expressed proteins, aforementioned nuclei-free INS-1 cell homogenates were centrifuged at 100000*g* for 60 min to obtain cytosol and pellets that contained all membrane and intact organelles. The pellets were resuspended in homogenization buffer and subjected to sonication to disrupt organelles. The resultant extracts were centrifuged again at 100000*g* for 60 min to separate the soluble luminal content of organelles (supernatant) from pure membrane fractions (sediments). Syncollin and insulin in each fraction were analyzed by Western blotting and radioimmunoassay, respectively.

Detection of Syncollin Expression by Western Blotting. Samples harvested from subcellular fractionation were denatured in treatment buffer at 95 °C for 5 min and separated on 15% polyacrylamide gel electrophoresis. The separated proteins were electrotransferred to nitrocellulose membranes (Bio-Rad). Blots were probed with anti-syncollin antiserum (1:200) or anti-c-Myc (clone 9E10) monoclonal antibodies (Roche Diagnostics) at a concentration of 2 μg/mL. After being blocked with 5% nonfat milk, the membranes were incubated with horseradish peroxidase-conjugated anti-rabbit or anti-mouse IgG antibodies (Santa Cruz) at a dilution of 1:1000. After the membranes had been soaked in an enhanced chemiluminescence development solution (Pierce), immunoreactive bands were visualized with a ChemiDo imaging system (Bio-Rad).

Separation and Detection of Proinsulin and Insulin by Nondenatured Western Blotting. Cell extracts were prepared under nondenatured conditions {extraction buffer [50 mM Tris-HCl (pH 7.4), 1% NP-40, 150 mM NaCl, 1 mM EDTA, and aprotinin, leupeptin, and pepstatin (1 μg/mL each)]}. Protein samples (20 μg each) were mixed with a nondenaturation loading buffer (no heating) and separated on 18% polyacrylamide gels (no SDS) by electrophoresis. The separated proteins were electrotransferred to PVDF mem-

branes (Bio-Rad). Blots were probed with anti-insulin monoclonal antibody (1:1000) (Sigma, catalog no. I-2018). This antibody recognizes both insulin and proinsulin, according to the supplier's information. After being blocked with 5% nonfat milk, the membranes were incubated with horseradish peroxidase-conjugated goat anti-mouse IgG antibody (Pierce) at a dilution of 1:1000. Following the enhanced chemiluminescence development, immunoreactive bands in the membranes were visualized after exposure to X-ray films (Fuji). In these experiments, negative and positive controls were provided by immunoblotting extracts of rat liver and rat pancreas that do not express proinsulin or insulin and that contain large levels of insulin, respectively.

Double-Staining Immunofluorescence. INS-1 cells transfected with c-Myc-tagged syncollin gene or its truncated form were used in the experiments. The cells cultured in coverslips were washed twice in PBS (pH 7.4) and fixed for 10 min at room temperature in 3.7% paraformaldehyde in PBS. Following two washes in PBS, the cells were permeabilized by a 10 min incubation in PBS containing 0.05−0.1% Triton X-100. After being blocked for 30 min in PBS containing 10% fetal calf serum, the cells were incubated overnight at room temperature in staining solution containing 1:20 diluted anti-c-Myc MAb (clone 9E10) (Roche Diagnostics) or anti-c-Myc polyclonal antibody (A14) (Santa Cruz), and also one of the following antibodies against organelle markers: mouse anti-insulin monoclonal antibody (Sigma) for secretory granules (1:500), rabbit anti-Mn^{2+} superoxide dismutase (MnSOD)[1] polyclonal antibody (StressGen, Victoria, BC) for mitochondria (1:500), anti-calnexin polyclonal antibody (Santa Cruz) for ER (1:100), and rabbit anti-α-mannosidase II antiserum (from K. Moremer, University of Georgia, Athens, GA) for Golgi apparatus (1:1000). Subsequently, the coverslips were washed six times in PBS, and then incubated for 1 h with TRITC-conjugated anti-mouse IgG antibody or FITC-conjugated anti-rabbit IgG antibody (1:100 dilution) (Sigma). Thereafter, coverslips were washed again six times in PBS and mounted on slides with fluorescence mounting medium (Dako). Samples were examined using a laser confocal microscopy (Zeiss laser scanning confocal microscope 410).

Ultrastructural Distribution of Syncollin by Immunoelectron Microscopy. Pellets of control and transfected INS-1 cells were washed twice in 0.1 M phosphate buffer, before a 5 min fixation at room temperature in 4% paraformaldehyde and 0.1% glutaraldehyde, followed by a 60 min fixation in 4% paraformaldehyde [all fixatives diluted in 0.1 M phosphate buffer (pH 7.4)]. The cells were washed three times in 0.1 M phosphate buffer, embedded in 12% gelatin, and cooled on ice. Small blocks of gelatin-embedded cell pellets were infused with 2.3 M sucrose, frozen in liquid nitrogen, and sectioned with an EMFCS cryoultramicrotome (Leica). Ultrathin sections were mounted on Parlodion-coated copper grids. The sections were processed by following a previously described protocol (*11*, *12*) which, in these experiments, included a 1 h exposure at room temperature to the anti-syncollin antibodies indicated above, diluted 1:50−100, and a 20 min exposure at room temperature to goat anti-rabbit antibodies conjugated to either 10 or 15 nm gold particles. Cryosections were screened and photographed in a CM10 electron microscope (Philips, Eindhoven, The Netherlands). As positive controls, sections of rat pancreas were exposed to the anti-syncollin antibody, resulting in an immunostaining of zymogen granules consistent with that previously reported (*13*). Negative controls included exposure of the sections of INS-1 cells to a preimmune serum from the same rabbit that was used to generate the anti-syncollin antibodies, or to only the gold-conjugated goat antibody. None of these incubations resulted in a sizable, specific staining of the sections.

Quantitation of Granules. For assessment of the number and distribution of secretory granules, we used the cryo sections that had been prepared for immunostaining of syncollin. For each type of transfected INS-1 cell, we photographed 40−60 randomly selected cell profiles featuring a nucleus. All photographs were taken at the original magnification of 21000×, printed at the final magnification of 63000×, and scored for the number of secretory granules (defined as single membrane-bound organelles with a homogeneous, usually electron-dense content). These organelles were further scored for their presence at the periphery of each cell profile (determined as a band of cytoplasm that is 0.3 μm thick, corresponding to a 1−2 granule diameter, immediately under the cell membrane). The proportion of peripheral granules, expressed as a percentage, was calculated by dividing the number of granules present in this area by the total number of granules per cell profile. The numerical density of secretory granules, expressed as the number of granules per square micrometer, was calculated by dividing the total number of granules by the area of each profile, which was measured using a ACECAD Professional graphic tablet connected to a Quantimet Leica 500+ system (Leica, Cambridge Ltd.). Mean ± SEM values and statistical comparisons were carried out by analysis of variance, as provided by the Statistical Package for Social Sciences (SPSS Inc., Chicago, IL).

Measurements of Insulin Secretion. Insulin secretion was determined in static incubations or during perfusions as described previously (*8*, *14*). For static incubations, INS-1 cells were seeded in 24-well culture plates and cultured for 3−4 days. After twice being washed with Krebs−Ringer−Hepes buffer (KRB) containing 129 mM NaCl, 4.8 mM KCl, 1 mM $CaCl_2$, 1.2 mM $MgSO_4$, 1.2 mM KH_2PO_4, 5 mM $NaHCO_3$, 2.8 mM glucose, and 10 mM HEPES (pH 7.4), the cells were preincubated for 30 min at 37 °C in 0.5 mL of KRB. Subsequently, the medium was replaced with 0.5 mL of KRB containing secretagogues, and the cells were incubated for an additional 30 min. The supernatants were removed for measurements of secreted insulin, and the attached cells were extracted with acid and ethanol for determination of insulin content. For perfusion experiments, 2×10^6 cells were placed in 5 μm filter chambers (Whatman) and the flow rate was set at 0.5 mL/min. After perfusion for 30 min with KRB containing 2.8 mM glucose to achieve stable basal secretory rates, cells were stimulated with a high level of glucose plus forskolin for three pulses each of 10 min. Insulin was assessed by radioimmunoassay kits (Linco). The results of insulin secretion were expressed as percentages

[1] Abbreviations: $[Ca^{2+}]_i$, cytosolic fee Ca^{2+} concentration; cAMP, cyclic AMP; EM, electron microscopy; MnSOD, Mn superoxide dismutase; SNARE, soluble *N*-ethylmaleimide-sensitive factor attachment protein receptor.

of insulin content to normalize the possible difference in the cell mass among individual experiments.

Determination of $[Ca^{2+}]_i$. Cytosolic free Ca^{2+} levels ($[Ca^{2+}]_i$) were determined as described previously (*15*). Transfected INS-1 cells were detached from the flasks by trypsinization and then kept in a spinner for 3 h for recovery. Subsequently, the cells were loaded with a fluorescent Ca^{2+} probe by incubation with 1 μM Fura-2/AM for 30 min at 37 °C. After being washed, cells were aliquoted and $\sim 2 \times 10^6$ cells in 2 mL of KRB were transferred to a cuvette. Stimuli were added to the cuvette after equilibration of cells at 37 °C for ~15 min. Fluorescence was recorded by a spectrofluorometer (Perkin-Elmer LS-50B), with excitation and emission wavelengths of 340 and 505 nm, respectively. Unless specified, the contaminating fluorescence from extracellular Fura-2 was assessed by adding 50 μM Mn^{2+} (which then was chelated by adding 100 μM diethylenetriaminepentaacetic acid) and was subtracted accordingly for each trace. Calibration of fluorescent signals into $[Ca^{2+}]_i$ values was carried out using a formula described previously (*15*).

Measurement of Membrane Potential. Membrane potential of INS-1 cells was monitored using a voltage-sensitive fluorescent probe, bisoxonol, as described previously (*15*). The anionic dye binds to the plasma membrane; its fluorescence is increased when cells are depolarized and is decreased when cells are hyperpolarized. Approximately 2×10^6 cells in KRB buffer were placed in a cuvette. Bisoxonol (final concentration, 100 nM) was added, and cells were left at 37 °C for ~20 min for equilibration. Fluorescence was recorded with excitation and emission wavelengths of 540 and 580 nm, respectively. For comparison and statistical analysis, the bisoxonol fluorescent signals were normalized by expression of results as the percentage of a near-maximal depolarization achieved by 34 mM KCl in each trace.

Statistical Analysis. Data are presented as mean ± SEM and statistically analyzed by Student's paired or unpaired two-tail *t* test.

RESULTS

Transfection of the Syncollin Vector and Truncated Syncollin Construct in INS-1 Cells Produces Products with Identical Molecular Masses but which Display a Differential Distribution in Subcellular Fractions. As expected, a strong signal for syncollin was detected in rat pancreas extracts (Figure 1A, lane 1). Syncollin was not detectably expressed in either control INS-1 cells (Figure 1A, lane 2) or insulin-secreting HIT-T15 cells (data not shown), as assessed by Western blotting using antiserum against a 13-residue peptide (residues 96−108) of rat syncollin, as well as by RT-PCR by using syncollin N-terminal sequence 5′-accatgtccccgctgtgcct-3′ and C-terminal sequence 5′-tcaatagcacttgcagtaga-3′ as forward and reverse primers, respectively. Transfection of INS-1 cells with either the intact syncollin gene or a construct only encoding its truncated form (lacking the N-terminal hydrophobic domain) expressed proteins with a similar molecular mass of approximately 16 kDa (Figure 1A, lanes 3 and 4). Preimmune serum failed to detect such a band (data not shown). In addition, loading a pool of equal amounts of syncollin products from both constructs on a 15% polyacrylamide gel only produced a single dominant band of ~16 kDa (data not shown).

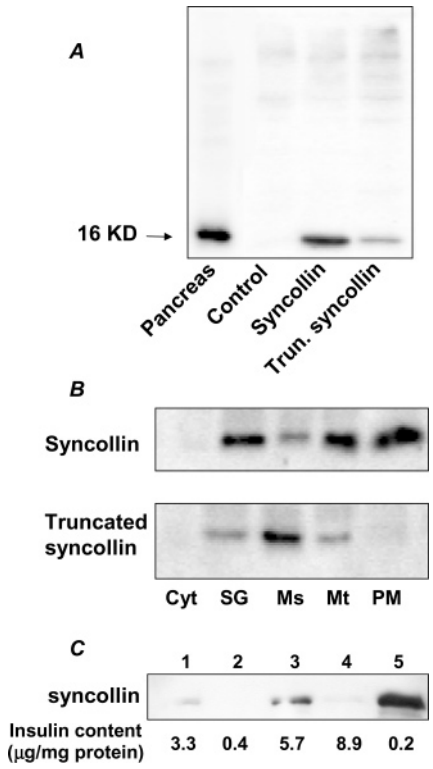

FIGURE 1: Distribution of expressed syncollin products in INS-1 cells. (A) Detection of syncollin in rat pancreas extracts and expression of transfected syncollin and truncated syncollin in INS-1 cell lysates by immunoblotting. (B) Detection of syncollin by immunoblotting in subcellular fractions. Cells were homogenized, followed by differential centrifugation to obtain cytosol (Cyt), mitochondria-rich (Mt), insulin granule-rich (SG), microsomal (MS), and plasmalemma-rich (PM) fractions. Equal amounts (20 μg) of proteins from each fraction were separated by SDS−PAGE and probed by an anti-syncollin serum. Data are representative of at least three experiments with identical results. (C) Examination of syncollin solubility and membrane association: lane 1, post-nuclear homogenates; lane 2, cytosol; lane 3, total membrane and organelles; lane 4, soluble content from organelles; and lane 5, total membranes after sonication. Results are representative of two independent experiments.

In our transfected INS-1 β-cell system, both products from the expression of either the complete syncollin gene or its truncated form were exclusively associated with the membrane-contained subcellular fractions when assessed by Western blotting (Figure 1B). For the former, strong signals were detected in the fractions rich with secretory granules or mitochondria, and also in the isolated plasma membrane, but with a weak signal in microsomes (Figure 1B). In contrast, the latter was detected mainly in microsomes, but only weakly in fractions rich with mitochondria or secretory granules. These results suggest that the N-terminal hydrophobic domain of syncollin may play an important role in directing the expressed product to the intracellular destinations.

The Product from Expression of the Intact Syncollin Gene Is Colocalized with Insulin Secretory Granules. The subcellular fractionation methods used in this study produce only organelle-enriched, but not sole, subcellular organelle fractions, since analysis of organelle markers in these fractions indicated cross contamination among them to various extents

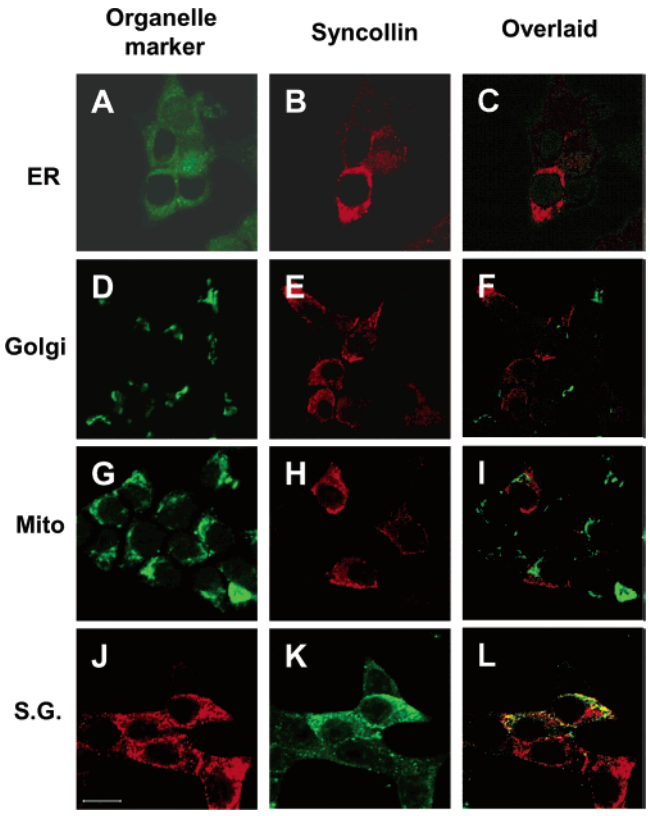

FIGURE 2: Intracellular colocalization of expressed syncollin in INS-1 cells. Expression of c-Myc-tagged syncollin in INS-1 cells was examined by immunofluorescence staining with anti-c-Myc monoclonal antibody and TRITC-conjugated anti-mouse IgG (B, E, and H) or anti-c-Myc polyclonal antibody and FITC-conjugated anti-rabbit IgG (K). ER was detected with the anti-calnexin polyclonal antibody and FITC-conjugated anti-rabbit IgG (A). The Golgi apparatus was detected with anti-α-mannosidase II antiserum and FITC-conjugated anti-rabbit IgG (D). Mitochondria were detected with the anti-MnSOD polyclonal antibody and FITC-conjugated anti-rabbit IgG (G). Secretory granules were detected with the anti-insulin monoclonal antibody and TRITC-conjugated anti-mouse IgG (J). Fluorescence was detected by laser confocal microscopy. Data are representative of at least three experiments with identical results: Mito, mitochondria; S.G., secretory granules. The bar is 10 μm.

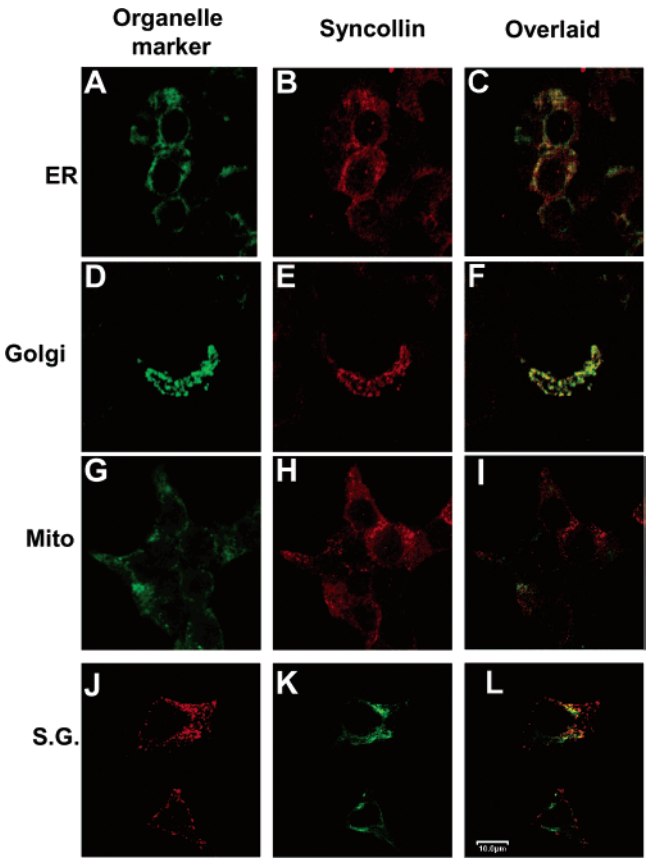

FIGURE 3: Intracellular colocalization of truncated syncollin in INS-1 cells. Expression of c-Myc-tagged truncated syncollin in INS-1 cells was examined by immunofluorescence staining with the anti-c-Myc monoclonal antibody and TRITC-conjugated anti-mouse IgG (B, E, and H) or the anti-c-Myc polyclonal antibody and FITC-conjugated anti-rabbit IgG (K). ER was detected with the anti-calnexin polyclonal antibody and FITC-conjugated anti-rabbit IgG (A). The Golgi apparatus was detected with anti-α-mannosidase II antiserum and FITC-conjugated anti-rabbit IgG (D). Mitochondria were detected with the anti-MnSOD polyclonal antibody and FITC-conjugated anti-rabbit IgG (G). Secretory granules were detected with the anti-insulin monoclonal antibody and TRITC-conjugated anti-mouse IgG (J). Data are representative of at least three experiments with identical results. Fluorescence was detected by laser confocal microscopy: Mito, mitochondria; S.G., secretory granules. The bar is 10 μm.

(*8*). Thus, we also examined the intracellular localization of expressed syncollin by double immunofluorescence staining. The results revealed that, in cells transfected with full-length c-Myc-tagged syncollin, the expressed protein is not colocalized with the markers of ER (calnexion; Figure 2A−C), Golgi apparatus (α-mannosidase II; Figure 2D−F), or mitochondria (MnSOD; Figure 2G−I). The only fluorescence signal colocalizing with syncollin is insulin, the marker of secretory granules (Figure 2J−L). On the other hand, the product from the truncated syncollin gene was found to colocalize with the marker of the Golgi apparatus (α-mannosidase II; Figure 3D−F), and partly with the marker of ER (calnexion; Figure 3A−C), but not with the markers of mitochondria (MnSOD; Figure 3G−I) or secretory granules (Figure 3J−L). These colocalization studies suggest that the syncollin signal in the mitochondria-enriched fraction detected using Western blotting (see above) could have resulted from contaminating insulin granules, since analyses of the organelle markers using this fraction from differential centrifugation revealed that it contains moderate insulin content (*8*). Thus, these observations together indicate that only the product from the intact syncollin gene is specifically distributed in the secretory granules of transfected INS-1 cells, pointing to an indispensable role of the N-terminal hydrophobic domain in this process.

Native syncollin in zymogen granules of pancreatic acinar cells is found both free in the lumen and bound to the membrane (*16*). In the syncollin-transfected INS-1 cells, the protein appeared exclusively to be associated with membranes (Figure 1C, lane 5) and not soluble in the lumen (Figure 1C, lane 4), as assessed by Western blotting after disruption of all organelles by sonication. This is in contrast to the distribution of insulin that was found primarily in the soluble fraction with little detectable in the pure membrane fraction (Figure 1C).

The ultrastructural distribution of ectopically expressed syncollin was also examined by immunoelectron microscopy. In control INS-1 cells, the anti-syncollin antibody resulted in a limited, spurious labeling of very few cells (data not shown). This level of labeling was markedly increased in

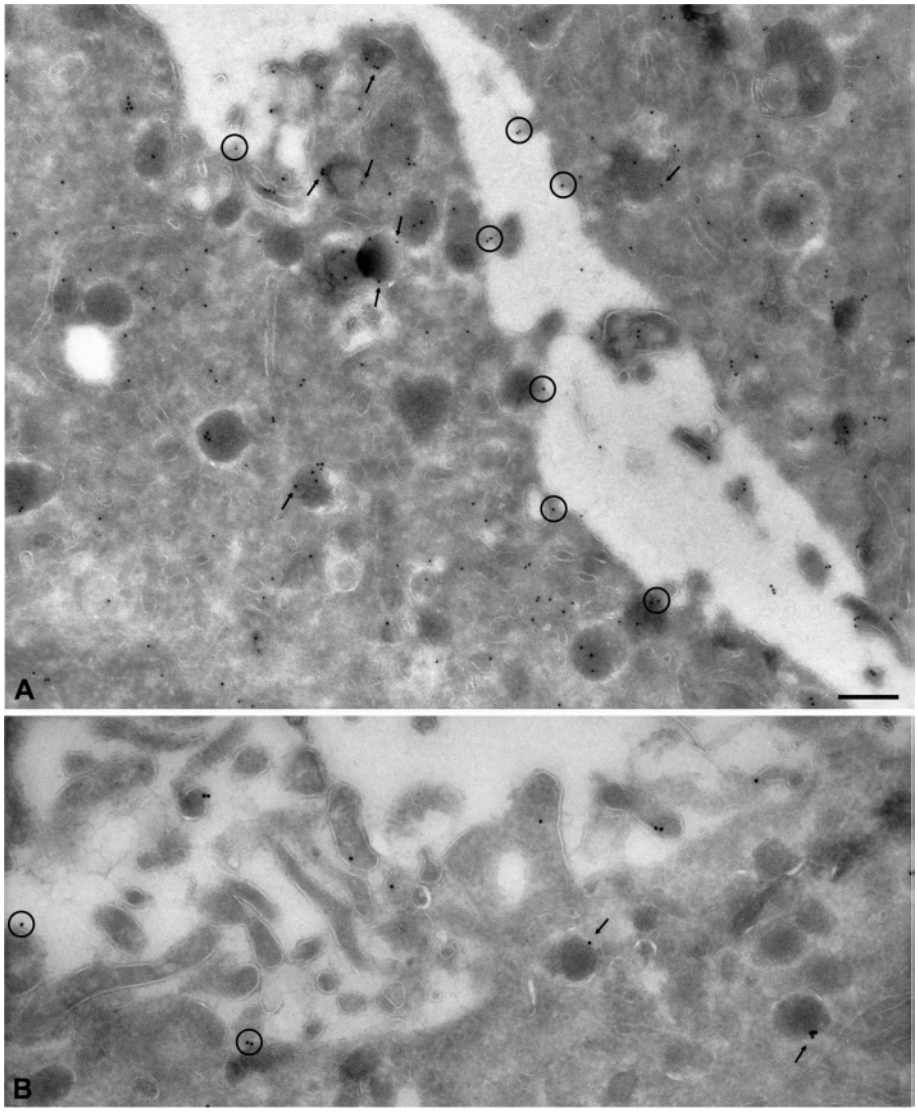

FIGURE 4: Ultrastructural distribution of syncollin in transfected INS-1 cells. (A) In INS-1 cells transfected for full-length syncollin, the immunolabeled protein was observed in tubular and vesicular organelles, over the luminal content of dense core secretory granules, and at the membrane of the latter organelles (arrows). Syncollin was also observed at discrete spots along the plasma membranes (circled) and on surface microvilli. (B) Under conditions of limited immunolabeling, syncollin was still observed at the membrane of secretory granules (arrows), as well as on both flat (circled) and microvillar regions of the cell membrane. The bar is 200 nm.

some, but not all, cells of the cultures that had been transfected for full-length syncollin. In these cells, the anti-syncollin antibody labeled multiple cytoplasmic compartments, including vesicular and tubular elements of the Golgi apparatus, and secretory granules (Figure 4A). Due to the small size of the latter organelles, the gold particles conjugated to the secondary antibody were variably observed over the dense content of the granules or at their membrane (Figure 4A). However, when the overall level of the immunolabeling was decreased by changing the concentration of the primary antibody and the size of the gold particles conjugated to the secondary antibody, the residual labeling for syncollin was mostly seen at the granule membrane (Figure 4B). Under all conditions, labeling for syncollin was also seen at the surface of microvilli of the cell membrane, as well as sites of this membrane facing secretory granules (Figure 4B). In addition, morphometric evaluation revealed that (1) the number of the granules featuring a dense insulin-containing core per square micrometer was not altered by syncollin expression and (2) the number of such granules that were located close to the cell membrane was comparable in control and transfected INS-1 cells (Table 1). Comparable observations were made in cultures transfected for truncated syncollin (Table 1), except that, in these cases, virtually no labeling of syncollin was seen over secretory granules and at the plasma membrane (data not shown).

Table 1: Secretory Granules of Syncollin-Transfected INS-1 Cells

INS-1 cell type	no. of cells	area (μm^2)	no. of granules	no. of granules/μm^2 [a]	% granules at the membrane[a]
control	40	4520	2597	0.57 ± 0.06	25 ± 4
truncated syncollin	58	6380	3364	0.52 ± 0.09	20 ± 6
full-length syncollin	46	5244	2760	0.53 ± 0.11	23 ± 6

[a] Data are the mean ± SEM of the indicated number of cell profiles.

Syncollin Expression Does Not Alter Insulin Biosynthesis and Conversion of Proinsulin to Insulin. The insulin content of INS-1 cells was not altered by stable transfection of either complete syncollin gene or its truncated form that lacks the

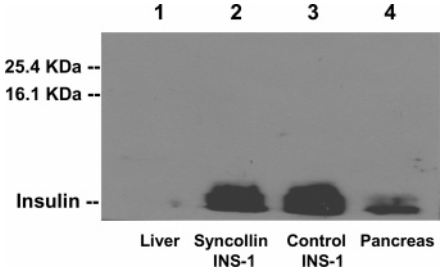

FIGURE 5: Separation and detection of proinsulin and insulin by nondenatured Western blotting. INS-1 cells and the negative (rat liver) and positive (pancreas) control tissues were extracted under nondenatured conditions. Samples (20 μg of protein) were subjected to nondenatured PAGE, followed by immunoblotting using an anti-insulin antibody which recognizes both proinsulin and insulin. However, only a single band could be detected in INS-1 cells and pancreas (the molecular markers are only just for rough reference, as they were run on nondenatured gels). Results are representative of four independent experiments.

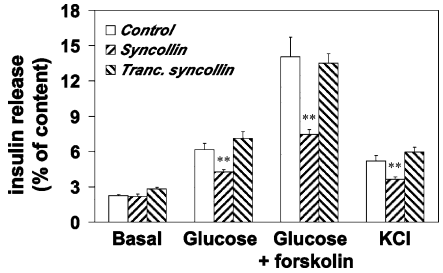

FIGURE 6: Inhibition of secretagogue-induced insulin secretion in INS-1 cells after transfection of full-length but not truncated syncollin. Cells were cultured in 24-well plates. After stimulation of cells by secretagogues for 30 min, insulin secretion and insulin content were assessed by RIA. Data are the mean ± SEM from four independent experiments in triplicate. The following concentrations were used: 15 mM glucose, 1 μM forskolin, and 34 mM KC1. Two asterisks indicate $P < 0.01$ vs control.

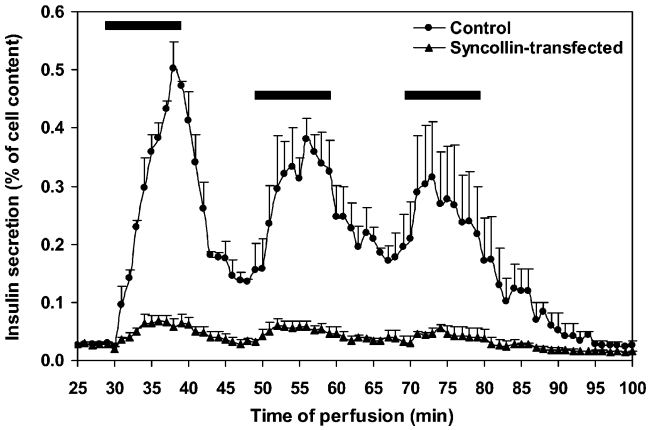

FIGURE 7: Transfection of intact syncollin gene-impaired glucose and forskolin-evoked insulin secretion in perfused INS-1 cells. Cells in suspension were first perfused for 30 min with nonstimulatory solution, and then challenged with 15 mM glucose and 1 μM forskolin three times as indicated by bars. The values of each point are the mean ± SEM from three observations: (●) control cells and (▲) cells transfected with the intact syncollin gene.

N-terminal hydrophobic domain [0.41 ± 0.03 (control), 0.42 ± 0.03, and 0.43 ± 0.04 ng/ng of DNA, respectively]. Proinsulin and insulin were separated and detected by nondenatured Western blotting. Negative (rat liver) and positive (rat pancreas) control samples were utilized to demonstrate the specificity of the insulin antibody that was used and to compare the proinsulin/insulin profile of INS-1 cells (with or without syncollin transfection) with that of the positive control. Only a single band at a low molecular mass range (much less than 16.1 kDa, the lowest marker applied) could be identified in INS-1 cells and rat pancreas, but not in rat liver (Figure 5). It appeared apparently that proinsulin levels were too low to be detectable in these samples. The predominant band obviously stands for insulin, since proinsulin is rapidly and efficiently converted into insulin in normal islet β-cells (*17*). The existence of a dominant insulin band in control INS-1 cells (Figure 5, lane 3) indicates that proinsulin is also efficiently converted into insulin, which was demonstrated previously in these cells by HPLC separation showing essentially only material coeluting with insulin I and II, with little if any immunoreactive proinsulin (*6*). Importantly, ectopic expression of syncollin did not alter the conversion of proinsulin into insulin (Figure 5, lane 2) in INS-1 cells, suggesting proinsulin sorting/maturation in the granules is not affected.

Insulin Release Simulated by Secretagogues Is Inhibited in INS-1 Cells Transfected with Syncollin but Not with Its Truncated Form. Ectopic expression of syncollin did not affect the basal insulin secretion in these cells (Figure 6). However, in cells transfected with full-length syncollin, the extent of insulin secretion, when stimulated by 15 mM glucose alone or combined with 1 μM forskolin (which increases the level of cAMP by directly stimulating adenylyl cyclase), was significantly decreased by 47 or 55%, respectively (Figure 6). High-level potassium (34 mM)-elicited insulin release (due to enhanced Ca^{2+} influx via depolarization) was also significantly inhibited by 48% in these cells. In contrast, transfection of INS cells with the truncated syncollin did not alter the insulin secretory responses to any of the same stimuli (Figure 6).

The effect of transfection of the complete syncollin gene on insulin secretion was also examined during perfusion of cells. Stimulation of control cells with 15 mM glucose and 1 μM forskolin for 10 min markedly increased the level of insulin release, while withdrawal of the stimulants caused a rapid decline of secretory rates (Figure 7). Two additional pulses of stimulation also evoked significant insulin secretory peaks, albeit to a slightly lesser extent. In contrast, the stimulated insulin secretion during the three pulses was markedly suppressed in syncollin-transfected cells, without affecting basal secretory rates (Figure 7).

To exclude a possible nonspecific effect of syncollin overexpression in INS-1 cells, we also transfected proline-rich acidic protein (PRAP) into INS-1 cells. PRAP had been found to be expressed in epithelial cells of gastrointestinal tract, liver, kidney, and pregnant uterus. The PRAP gene encodes a protein with 151 amino acids, and as in syncollin, its 20 N-terminal amino acids have been predicted to serve as a signal peptide, suggesting that PRAP is a secreted protein sorted into secretory granules (*18*). However, no significant alteration of insulin secretory responses to glucose and other stimulants was observed in PRAP-transfected INS-1 cells (data not shown).

Expression of Syncollin Does Not Affect Membrane Depolarization or $[Ca^{2+}]_i$ Elevation. Since the expression of syncollin in INS-1 cells produced a general inhibition of regulated insulin secretion, possible alterations in the generation of proximal signals for the stimulus−secretion coupling

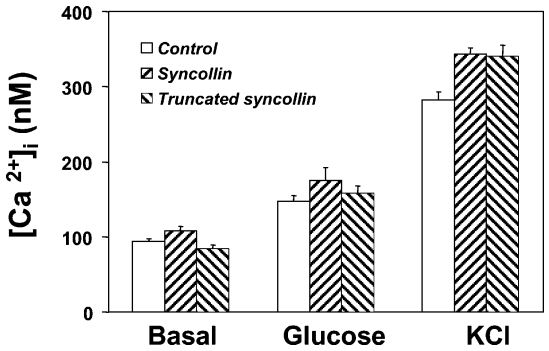

FIGURE 8: Glucose and high K^+-evoked $[Ca^{2+}]_i$ increases were not reduced in syncollin-expressed INS-1 cells. $[Ca^{2+}]_i$ levels in INS-1 cells were measured by loading a fluorescent Ca^{2+} probe (Fura-2) as described in detail in Materials and Methods. Values are the mean ± SEM from three independent experiments. The following concentrations were used: 15 mM glucose and 34 mM KCl.

were examined. We found that glucose-induced membrane depolarization was not altered in INS-1 cells transfected with syncollin (data not shown). Moreover, the $[Ca^{2+}]_i$ elevations evoked by either high glucose or high K^+ levels were also not reduced in these cells. In fact, the response to the latter stimulus might have been slightly augmented (Figure 8). Together, these data suggest that syncollin localized in insulin granules may inhibit insulin secretion at late stages in the exocytotic cascade.

DISCUSSION

In this study, we ectopically expressed syncollin in an intact cell system of exocytosis to investigate the effect of this protein on regulated secretion. Our results revealed that insulin secretion induced by several well-known secretagogues was significantly inhibited by the expression of syncollin in INS-1 β-cells. Importantly, this effect is dependent on the existence of the N-terminal hydrophobic domain of the protein (which though is apparently removed post-translationally), since transfection of a truncated syncollin lacking this domain did not modify stimulated insulin release. Our data also indicate that targeting of syncollin to secretory granules is necessary to affect stimulated insulin secretion. There was neither alteration of insulin biosynthesis and proinsulin conversion to insulin nor any impairment of the generation of the proximal signals (membrane depolarization and increase in $[Ca^{2+}]_i$) required for triggering exocytosis of insulin granules, pointing to an action on the distal steps of exocytosis.

The expressed products from transfection of both syncollin and its truncated form are membrane- or organelle-associated, noncytosolic proteins, as assessed by subcellular fractionation followed by Western blotting. However, the N-terminal hydrophobic domain influenced the intracellular distribution of syncollin. Moreover, this hydrophobic domain in the full-length syncollin-transfected INS-1 cells is apparently removed during the processing after translation, since the proteins detected in these cells displayed a molecular mass similar to that in the cells transfected with the truncated form lacking this domain (cf. Figure 1A). In the course of carrying out this study, the biochemical properties of syncollin have been further characterized by other laboratories. Studies using pancreatic acinar cells revealed that the full-length syncollin has a cleavable signal sequence (*5*). Therefore, it is obvious that the final protein products from the two syncollin constructs in INS-1 cells are almost identical and lack an N-terminal hydrophobic domain. This conclusion is also supported by our observation that the both products are indistinguishable on a 15% gel which is capable of separating a difference in molecular mass of 2 kDa equivalent to the N-terminal hydrophobic domain.

Endogenous syncollin in exocrine acinar cells was found to be a protein in the zymogen granule (*1*, *5*). In our transfected INS-1 β-cell system, the expressed syncollins from both constructs (full and its truncated form lacking the N-terminal hydrophobic domain) were exclusively associated with the membranes. However, immunofluorescence studies revealed different intracellular targeting: a colocalization of syncollin staining specifically with insulin (indicative of secretory granules) in cells transfected with full-length syncollin, but not in cells transfected with a truncated form. In the case of the latter, expressed syncollin was colocalized mainly with the Golgi apparatus and also partly with ER. The observations from immuno-EM were consistent with the immunofluorescence findings. These results suggest that the expressed full-length syncollin in INS-1 cells can be sorted to secretory granules as in pancreatic acinar cells (*2*, *5*). It is apparent that the N-terminal hydrophobic domain serves as the signal peptide in this case and is essential for syncollin sorting to secretory granules in both exocrine and endocrine cells. In a study by Hodel and Edwardson in which the intracellular targeting of syncollin was examined, it was found that both GFP- and His_6-tagged (at C-terminal) syncollin proteins from transfection are sorted to the vesicles in both AtT-20 cells and AR42J cells (*19*). Interestingly, His_6-tagged syncollin is efficiently targeted to secretory granules only in the former but not in latter cells, whereas GFP-tagged syncollin is identified in the secretory granules of both types of cells (*19*). Such a difference between His_6- and GFP-tagged syncollin in sorting into secretory granules may be explained by the tendency of GFP (upon being linked to a signal peptide) to enter granules (*20*).

Our further studies of subcellular fractions on syncollin targeting (cf. Figure 1C) revealed that the expressed syncollin in insulin granules is not a soluble protein in the lumen but rather that is bound to the granule membrane. By purposely limiting the level of immunolabeling at the ultrastructural level, we could preferentially visualize the localization of syncollin at the insulin granule membrane. This is in contrast to the situation in pancreatic acinar cells where syncollin was found in both the lumen and membrane of zymogen granules (*13*). This might be attributable to possible difference in the membrane composition between the two types of granules (see below). Although the exact mechanism is unclear, the ability of syncollin to associate with membranes may be due to its ability to form a hydrophobic structure probably via homo-oligomerization (*13*, *16*), though the monomer lacks a hydrophobic domain. The native syncollin in pancreatic acinar cells appeared to be associated with special membrane lipid microdomains in zymogen granules (*16*, *21*). This feature of the membrane association of syncollin homo-oligomers may involve its interaction with cholesterol and other membrane contents such as GPI (*5*, *13*). In addition, our data suggest that the syncollin synthesized following the transfection of the full-length construct

is bound to the inner leaflet of granule membrane, which can be explained by the distinct intracellular localization of the products from the two syncollin constructs. The protein from transfection of the construct encoding the truncated syncollin is associated with the Golgi apparatus and ER, but not with insulin granules, despite its similar property of membrane association. Such targeting may result from possibly higher levels of cholesterol or other lipids in some microdomain of the Golgi and ER membrane, which might favor syncollin interaction at those sites. Since truncated syncollin lacks an N-terminal hydrophobic domain (the signal sequence) during translation, it will not enter into the lumen from ER into the insulin granules. Therefore, they can be exposed to only the outer leaflet of organelles, including insulin granules. However, such cytosolic syncollin did not bind to insulin granules, in contrast to the luminal syncollin in the granules. These results thus also imply a difference in the membrane composition (which affects syncollin association) between insulin granules and the ER/Golgi apparatus, as well as between inner and outer leaflets of insulin granule membranes. Such a difference in membrane composition among various organelles and the asymmetry of bilayer membranes do occur in the cell (*22*, *23*).

Our data indicate that the inhibitory effect of syncollin on insulin release occurs in the late stage of the secretion process, since the generation of the proximal stimulus−secretion coupling signals (membrane depolarization and $[Ca^{2+}]_i$ elevation) was not affected and the insulin secretion evoked by the stimuli tested, including a high level of K^+ (presumably a pure Ca^{2+} stimulation), was also impaired. The fact that inhibition of stimulated insulin secretion occurs in only the cells transfected with full-length syncollin, but not in the cells expressing the truncated syncollin missing the hydrophobic domain (signal peptide), indicates that syncollin sorting to secretory granules is necessary to affect regulated insulin secretion. Transfection of syncollin in rat islets also inhibited insulin secretion in a preliminary study by other laboratories (*24*). Furthermore, it appears that association of syncollin with granule membranes is required for its inhibitory effect of regulated insulin secretion, since GFP-tagged syncollin, which exists as a free soluble protein in the lumen of granules, had no such action (*25*). Further studies using mutated or partially deleted syncollin constructs (other than N-terminally truncated one) to transfect cells may pinpoint the domain(s) responsible for its sorting into granules and its inhibitory effect on insulin secretion.

Sorting syncollin into insulin granules seems not to affect granule trafficking, since repeated stimulation with glucose and forskolin produced a similar extent of reduction of acute insulin secretion in syncollin-transfected cells (cf. Figure 7). It is more likely that syncollin, when bound to the granule membrane, inhibits insulin secretion by impeding a very late step in exocytosis, i.e., granule fusion and/or docking, given the fact that the regulated secretion by the first pulse of stimulation was already dramatically suppressed (cf. Figure 7). The inhibitory effect of syncollin on stimulated insulin secretion may be related to its specific location and its unique molecular property (i.e., strong membrane association feature in the form of homo-oligomers which may interact with other lipids and proteins in the secretory granules). For instance, syncollin-associated membrane rafts contain not only GP-2, a major glycosylphosphatidylinositol (GPI)-anchored membrane glycoprotein which is believed to be a sortase, but also the members of v-SNAREs such as synaptobrevin-2 in acinar cells (*13*). Integration of syncollin homo-oligomers in the granule membrane may also change the lipid composition of its bilayers. It is known that exocytosis involve not only proteins but also phospholipids in the implicated membranes (*26*−*28*). When our work was being submitted for publication, a study on AtT-20 cells reported a 45% reduction in secretory vesicles in the region at the tips of cell processes after ectopic expression of syncollin, which could explain the reduction of the level of stimulated ACTH release to a similar extent (*29*). However, this mechanism may not apply to our study, since we did not find significant alteration in the total insulin content and proinsulin biosynthesis in our syncollin-expressed cells and the results from electron microscopy examination also could not detect a difference between control and syncollin-transfected INS-1 cells in the number of either total insulin-containing granules or those granules that were located close to the cell membrane (cf. Table 1). It is worth mentioning that syncollin labeling was observed over microvilli, as well as over membrane domains facing marginating granules in these cells. Alternatively, the inhibitory effect on insulin secretion of ectopic expression of syncollin might result from a blockage of the conversion of proinsulin to insulin. Such a scenario is, however, not supported by our data from the experiments of nondenatured Western blotting which was unable to detect a change in proinsulin and insulin contents after syncollin expression (cf. Figure 5). Taken together, it is anticipated that syncollin interferes with stimulated secretion at a stage somewhere between insulin granule docking and its membrane fusion in INS-1 cells, possibly by disturbing the granule membrane composition and/or structure required for exocytosis.

The physiological function of syncollin remains to be defined. Besides its existence in pancreatic acinar cells, syncollin has also been found to be expressed in small intestine and parotid gland (*1*, *2*), and its expression is inducible (*2*). These observations imply that syncollin is a protein related to secretion of digestion enzymes in exocrine cells. The sorting of syncollin into zymogens suggests that syncollin may be involved in the processing of zymogen content in exocrine cells. However, syncollin-knockout mice did not display any abnormal phenotype either in zymogen contents or in regulated secretion, and only exhibited weaker stress responses (*3*). Nonetheless, its possible physiological role in regulated secretion cannot be completely ruled out. In fact, a recent study claimed that different results were obtained using the same knockout mice, in which the level of secretagogue-stimulated amylase release was reduced by 50%, the number of individual exocytotic events was also reduced to the same extent, and delivery of newly synthesized protein to zymogen granules was delayed (*29*), suggesting that syncollin might play a role in exocytosis in pancreatic acinar cells. Therefore, the findings from our studies and by others indicate that syncollin may be involved in regulated secretion in the cell. However, the physiological relevance of syncollin or its possible analogous protein in β-cells remains unsolved.

ACKNOWLEDGMENT

We are grateful to Ms. Fei Xie for skillful technical assistance. Portions of this work were published as an abstract

at the 62nd Annual Meeting of the American Diabetes Association (San Francisco, CA, June 2002). We thank Dr. Stewart A. Metz for editorial assistance with the manuscript.

REFERENCES

1. Edwardson, J. M., An, S., and Jahn, R. (1997) The secretory granule protein syncollin binds to syntaxin in a Ca^{2+}-sensitive manner, *Cell 90*, 325−333.
2. Tan, S., and Hooi, S. C. (2000) Syncollin is differentially expressed in rat proximal small intestine and regulated by feeding behavior, *Am. J. Physiol. 278*, G308−G320.
3. Antonin, W., Wagner, M., Riedel, D., Brose, N., and Jahn, R. (2002) Loss of the zymogen granule protein syncollin affects pancreatic protein synthesis and transport but not secretion, *Mol. Cell. Biol. 22*, 1545−1554.
4. Imai, A., Nashida, T., and Shimomura, H. (2001) mRNA expression of membrane-fusion-related proteins in rat parotid gland, *Arch. Oral Biol. 46*, 955−962.
5. An, S. J., Hansen, N. J., Hodel, A., Jahn, R., and Edwardson, J. M. (2000) Analysis of the association of syncollin with the membrane of the pancreatic zymogen granule, *J. Biol. Chem. 275*, 11306−11311.
6. Asfari, M., Janjic, D., Meda, P., Li, G. D., Halban, P. A., and Wollheim, C. B. (1992) Establishment of 2-mercaptoethanol-dependent differentiated insulin-secreting cell lines, *Endocrinology 130*, 167−178.
7. Poitout, V., Olson, L. K., and Robertson, R. P. (1996) Insulin-secreting cell lines: Classification, characteristics and potential applications, *Diabetes Metab. 22*, 7−14.
8. Li, G. D., Kowluru, A., and Metz, S. A. (1996) Characterization of prenylcysteine methyltransferase in insulin-secreting cells, *Biochem. J. 316*, 345−351.
9. Graham, J. M. (1997) in *Subcellular fractionation: A practical approach* (Graham, J. M., and Rickwood, R., Eds.) pp 205, Oxford University Press, Oxford, U.K.
10. Hubbard, A. L., Wall, D. A., and Ma, A. (1983) Isolation of rat hepatocyte plasma membranes. I. Presence of the three major domains, *J. Cell Biol. 96*, 217−229.
11. Liou, W., Geuze, H. J., and Slot, J. W. (1996) Improving structural integrity of cryosections for immunogold labeling, *Histochem. Cell Biol. 106*, 41−58.
12. Tokuyasu, K. (1997) in *Cells, a laboratory manual: Subcellular localization of genes and their products* (Spector, D., Goodman, R., and Leinwand, L., Eds.) Vol. 3, pp 131.1−131.27, Cold Spring Harbor Laboratory Press, Plainview, NY.
13. Kalus, I., Hodel, A., Koch, A., Kleene, R., Edwardson, J. M., and Schrader, M. (2002) Interaction of syncollin with GP-2, the major membrane protein of pancreatic zymogen granules, and association with lipid microdomains, *Biochem. J. 362*, 433−442.
14. Li, G. D., Rungger-Brandle, E., Just, I., Jonas, J. C., Aktories, K., and Wollheim, C. B. (1994) Effect of disruption of actin filaments by *Clostridium botulinum* C2 toxin on insulin secretion in HIT-T15 cells and pancreatic islets, *Mol. Biol. Cell 5*, 1199−1213.
15. Li, G. D., Luo, R. H., and Metz, S. A. (2000) Effects of inhibitors of guanine nucleotide synthesis on membrane potential and cytosolic free Ca^{2+} levels in insulin-secreting cells, *Biochem. Pharmacol. 59*, 545−556.
16. Hodel, A., An, S. J., Hansen, N. J., Lawrence, J., Wasle, B., Schrader, M., and Edwardson, J. M. (2001) Cholesterol-dependent interaction of syncollin with the membrane of the pancreatic zymogen granule, *Biochem. J. 356*, 843−850.
17. Rhodes, C. J., and Halban, P. A. (1987) Newly synthesized proinsulin/insulin and stored insulin are released from pancreatic B cells predominantly via a regulated, rather than a constitutive, pathway, *J. Cell Biol. 105*, 145−153.
18. Zhang, J., Wong, H., Ramanan, S., Cheong, D., Leong, A., and Hooi, S. C. (2003) The proline-rich acidic protein is epigenetically regulated and inhibits growth of cancer cell lines, *Cancer Res. 63*, 6658−6665.
19. Hodel, A., and Edwardson, J. M. (2000) Targeting of the zymogen-granule protein syncollin in AR42J and AtT-20 cells, *Biochem. J. 350* (Part 3), 637−643.
20. Molinete, M., Lilla, V., Jain, R., Joyee, P. B. M., Gorr, S.-U., Ravazzola, M., and Halban, P. A. (2000) Trafficking of non-regulated secretory proteins in insulin secreting (INS-1) cells, *Diabetologia 43*, 1157−1164.
21. Geisse, N. A., Wasle, B., Saslowsky, D. E., Henderson, R. M., and Edwardson, J. M. (2002) Syncollin homo-oligomers associate with lipid bilayers in the form of doughnut-shaped structures, *J. Membr. Biol. 189*, 83−92.
22. van Meer, G. (2000) Cellular organelles: How lipids get there, and back, *Trends Cell Biol. 10*, 550−552.
23. Keenan, T. W., and Morre, D. J. (1970) Phospholipid class and fatty acid composition of golgi apparatus isolated from rat liver and comparison with other cell fractions, *Biochemistry 9*, 19−25.
24. Hays, L. B., Wicksteed, B., Mccuaig, J., Halban, P. A., Philipson, L. H., Edwardson, J. M., and Rhodes, C. J. (2002) Intragranular Factors Influence Regulated Insulin Exocytosis, *Diabetes 51* (Suppl. 2), A368.
25. Ma, L., Bindokas, V. P., Kuznetsov, A., Rhodes, C., Hays, L., Edwardson, J. M., Ueda, K., Steiner, D. F., and Philipson, L. H. (2004) Direct imaging shows that insulin granule exocytosis occurs by complete vesicle fusion, *Proc. Natl. Acad. Sci. U.S.A. 101*, 9266−9271.
26. Martin, T. F. (1998) Phosphoinositide lipids as signaling molecules: Common themes for signal transduction, cytoskeletal regulation, and membrane trafficking, *Annu. Rev. Cell Dev. Biol. 14*, 231−264.
27. Metz, S. A. (1988) Membrane phospholipid turnover as an intermediary step in insulin secretion. Putative roles of phospholipases in cell signaling, *Am. J. Med. 85*, 9−21.
28. Bankaitis, V. A., and Morris, A. J. (2003) Lipids and the exocytotic machinery of eukaryotic cells, *Curr. Opin. Cell Biol. 15*, 389−395.
29. Wasle, B., Hays, L. B., Rhodes, C. J., and Edwardson, J. M. (2004) Syncollin inhibits regulated corticotropin secretion from AtT-20 cells through a reduction in the secretory vesicle population, *Biochem. J. 380*, 897−905.

BI048894D